Heliyon 11 (2025) e41906

Contents lists available at ScienceDirect

Heliyon

journal homepage: www.cell.com/heliyon

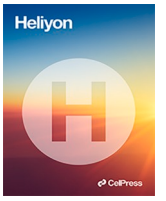

Research article

Network pharmacology and molecular analysis of mechanisms underlying the therapeutic effects of Rhubarb in treating atherosclerosis and abdominal aortic aneurysm

Huilin Xu [a], Jun Huang [a], Youjie Zeng [b], Xia Wang [a], Huilin Lian [a], Siyi Zhang [a], Ren Guo [a,*]

[a] Department of Pharmacy, The Third Xiangya Hospital, Central South University, Changsha, 410013, Hunan, China
[b] Department of Anesthesiology, Third Xiangya Hospital, Central South University, Changsha, 410013, Hunan, China

ARTICLE INFO

Keywords:
Rhubarb
Atherosclerosis
Abdominal aortic aneurysm
Cyberpharmacology
Traditional Chinese medicine
Computational biology
Molecular docking technology

ABSTRACT

Aim of the study: The aim of this study was to systematically investigate the effects and mechanisms of Rhubarb in the treatment of Atherosclerosis (AS) and Abdominal Aortic Aneurysm (AAA) by utilizing network pharmacology and molecular docking techniques.
Materials and methods: TCMSP systematic pharmacology database was utilized to search for active chemical components of Rhubarb. Disease-related targets were retrieved from the GEO dataset and Disgenet database. Gene interactions were utilized to identify common targets of Rhubarb with AS/AAA, and interaction networks were constructed using Cytoscape 3.9.1. Protein-protein interaction (PPI) networks for the core targets were constructed using the STRING database. GO and KEGG pathway enrichment analysis was performed using DAVID. Molecular docking is used to assess the potential target-active compound interactions.
Results: In our study, 16 active compounds were screened from Rhubarb, along with 310 targets. Additionally, 110 AS/AAA target genes were screened out. Topological analysis of the PPI protein network yielded 23 core targets. The targets, biological functions and signaling pathways of Rhubarb in AS/AAA were further investigated. The analysis indicated that Rhubarb may be effective in treating AS/AAA through processes such as lipids, atherosclerosis, extracellular matrix catabolism, collagenolytic metabolic processes, and the extracellular environment. Five core pharmacological targets were also identified: TNF, IL-1β MMP9, TP53, and PPARG. Molecular docking showed a strong binding ability between the active compounds and the screened targets.
Conclusions: This study successfully predicted the molecular functions, pharmacological targets, and pathways associated with Rhubarb for treating AS/AAA. In addition, identified potential active ingredients can be used as a source for AS/AAA drug screening.

1. Introduction

Cardiovascular disease, encompassing ischemic and hemorrhagic conditions of the heart, brain, and other organs, is the leading cause of mortality worldwide([1]; G [2]).This disease primarily results from hypertension, hyperlipidemia, diabetes mellitus, and

* Corresponding author. Department of Pharmacy, The Third Xiangya Hospital, Central South University, Changsha, 410013, Hunan, China.
E-mail address: pharmguor@csu.edu.cn (R. Guo).

https://doi.org/10.1016/j.heliyon.2025.e41906
Received 6 August 2024; Received in revised form 7 January 2025; Accepted 10 January 2025
Available online 23 January 2025

Abbreviations

TCM	Traditional Chinese Medicine;
AS	Atherosclerosis
AAA	Abdominal Aortic Aneurysm
PPI	Protein-Protein Interaction
GO	Gene Ontology
KEGG	Kyoto Encyclopedia of Genes and Genomes
TNF	Tumor Necrosis Factor
IL-1β	Interleukin 1, Beta
MMP9	Matrix Metallopeptidase 9
TP53	Tumor Protein P53
PPARG	Peroxisome Proliferator-Activated Receptor Gamma

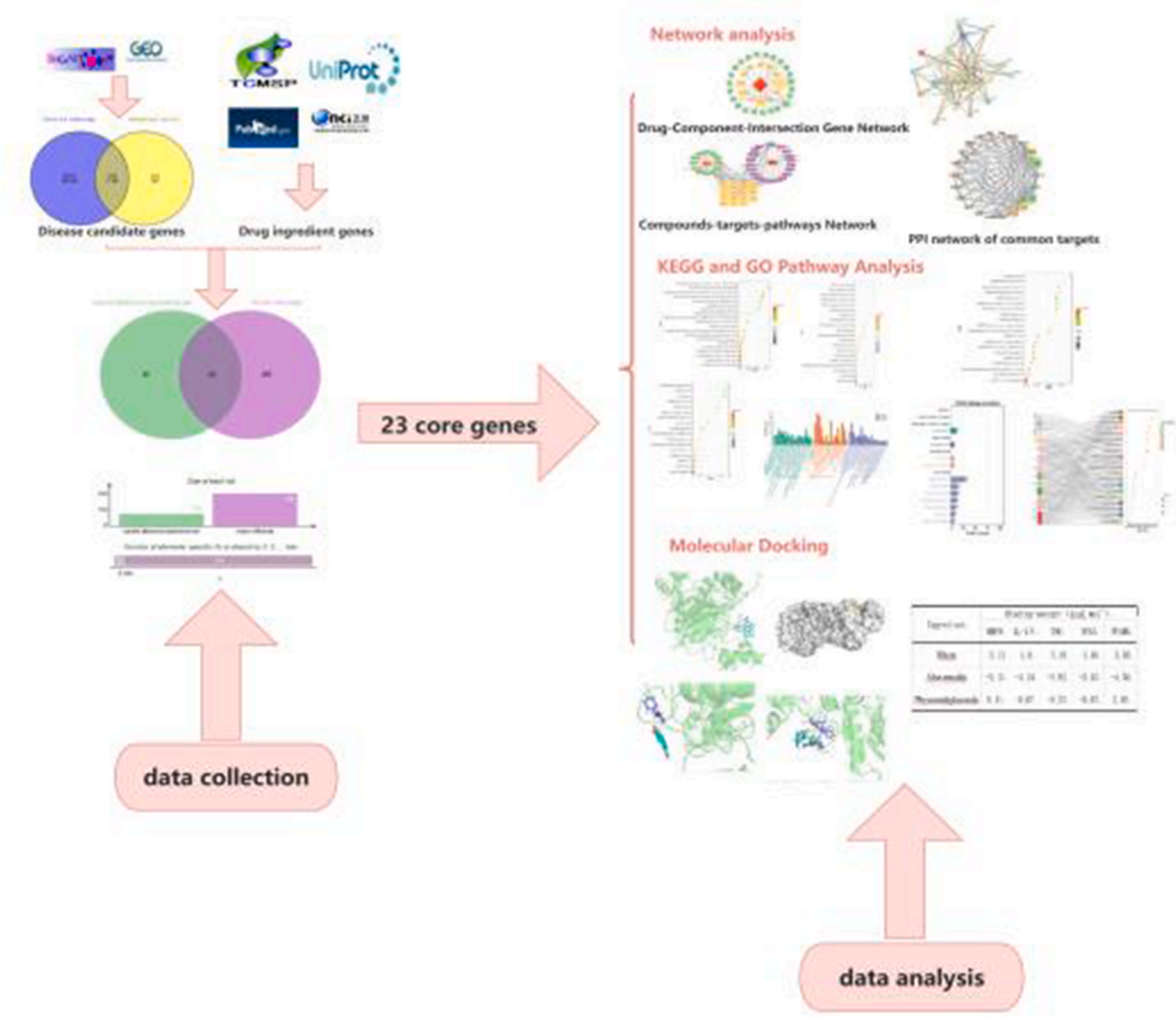

Fig. 1. Overall workflow of the study.Includes database preparation, network analysis, KEGG and GO pathway analysis and molecular docking four sections.

other conditions[3]. Atherosclerosis, a systemic inflammatory disease, predominantly affects medium to large arteries such as the aorta, carotid, iliac, and coronary arteries, and significantly contributes to cardiovascular disease([4]; [5]). Additionally, atherosclerosis is the leading cause of abdominal aortic aneurysms[4]. The progression of atherosclerosis is gradual, beginning with the appearance of lipid streaks on the abdominal aorta and eventually leading to plaque formation[6]; [7]. The repeated impact of arterial blood flow on the weak area in the middle of the plaque causes a tumor-like expansion, resulting in the outward expansion of the entire vessel wall[8]; [9]. If the bulge exceeds 50 % of the abdominal aortic wall, it is classified as an abdominal aortic aneurysm.

Rhubarb, derived from the dried root and rhizome of Polygonum palmatum L., Rheum tanguticum Maxim. ex Balf., or Rheum officinale Baill., possesses a cold nature and bitter taste, and is associated with the meridians of the spleen, stomach, large intestine, liver, and pericardium[10,11]. Its medicinal properties include alleviating diarrhea, reducing heat and inflammation, cooling and detoxifying the blood, resolving blood stasis, and regulating menstruation, and eliminating dampness and discoloration[12]. Consequently, Rhubarb is frequently employed as a Chinese herbal medicine in clinical settings. Recent pharmacological investigations have demonstrated the clinical efficacy of rhubarb in enhancing gastrointestinal functionality, halting hemorrhages, protecting cardiovascular and cerebral vasculature, and exerting anti-inflammatory, anti-bacterial, and anti-tumoral properties, among others[13,14]. This botanical agent is frequently employed to stimulate blood circulation and alleviate blood stasis. Accoding to the Divine Husbandman's Classic of the Materia Medica, rhubarb is employed to alleviate blood stasis and blood closure, as well as to disperse miasmatic impediments and accumulations[15]. It is widely used as a medicinal remedy to promote blood circulation and eliminate blood stasis.

Cyberpharmacology is a new field of study that investigates disease mechanisms and drug action within the broader context of biological networks[16]. The objective of network pharmacology research is to systematically explain scientific puzzles across multiple levels [17]. This theory is very similar to the main concepts of TCMSP disease treatment, the identification and treatment based on evidence[18].It employs an approach to predict the active ingredients of compounds and disease targets at a systemic level, and to establish multilevel networks such as drug-component-target-disease[19]. Molecular docking is a computer simulation technique that simulates interactions between molecules and proteins at the atomic level[20]. It predicts the conformations of ligands and receptors and calculates parameters such as binding energy, which can be used to assess the in vivo binding potential of drugs[21].

Due to the serious threat AAA poses to human life and health, it is important to validate the findings regarding atherosclerosis as the causative agent for AAA development. Therefore, our study aims to confirm the potential use of Rhubarb in treating AS/AAA through network pharmacology and molecular docking. The flow diagram of this study is shown in Fig. 1.

2. Materials and methods

2.1. Data collection

2.1.1. Screening of AS/AAA-related targets

The Gene Expression Omnibus dataset (GEO: www.ncbi.nlm.nih.gov/geo/) was searched for differentially expressed genes (GSE43292) in AS patients and in normal subjects. R software were used for multi-chip joint analysis, with batch correction. Differentially expressed genes (DEGs) were identified with a threshold of $P < 0.01$.Visualization of volcano and box plots was generated using the ggplot2 R package. AAA-associated disease targets were collected from Disgenet databases (https://www.disgenet.org/), using "Abdominal Aortic Aneurysm" as the keyword. Only target genes from the DisGeNET database with a score greater than 0.01 were considered as candidates. Finally, duplicate target genes were removed to create the AS/AAA gene library.

2.1.2. Screening of rhubarb active ingredients and prediction of target sites

The key search term "DaHuang" was used to obtain all components of Rhubarb in the TCMSP database (https://old.tcmsp-e.com/tcmsp.php). Oral bioavailability (OB) $\geq$30 % and drug-likeness (DL) $\geq$0.18 of Rheum palmatum were set as the screening criteria. Subsequently, searched protein names were converted to gene names using the UniProt database(http://www.UniProt.org/).

2.1.3. Component genes are intersected with disease targets

The constituent targets of AS/AAA and Rhubarb were entered into the drawing software, Draw Venn Diagram, to obtain a Venn diagram showing the potential targets of rhubarb against AS/AAA and their intersections.

2.2. Construction of PPI (protein-protein interaction networks network), screening the core targets

Cross-targets of herbal medicine and disease were imported into the STRING database (https://string-db.org), and a PPI network model was constructed with "*Homo sapiens*" as the biological species, with the unconnected nodes hidden and the rest of the parameters set to default values. The results were then imported into Cytoscape 3.9.1 for visualization. Key genes were filtered by Degree, Closeness, Betweenness, and Eigenvector using the CytoNCA plug-in.

2.3. Gene ontology and kyoto encyclopedia of genes and Genomes analyses

GO and KEGG analysis were performed to characterize and annotate the functions of the intersecting target genes and the potential signaling pathways. The intersecting target genes were channeled into the DAVID comprehensive database, selecting *Homo sapiens* as the species. The molecular function (MF), biological process (BP), and cellular component (CC) from the GO and KEGG analyses were

performed and the data were downloaded accordingly. The analyzed data were imported into the microbiome platform(https://www.bioinformatics.com.cn/) to create an enriched bubble map for visualizing structures.

2.4. Construction of the network

2.4.1. Construction of "drug-component-gene target" visualization reticulation

In order to clearly and unambiguously observe the relationship between components and targets, the intersecting target genes were imported into Cytoscape 3.9.1 software to visualization and analysis to construct a network diagram of drug-active ingredient-gene target interactions.

2.4.2. Construction of "Disease-KEGG pathway-target-component-drug" network

Data related to the active ingredients of Rhubarb, the intersecting target genes of traditional Chinese medicine-disease, and the top 20 KEGG pathways sorted by P-value were imported into Cytoscape 3.9.1 software. Subsequently, the disease-KEGG pathway-target-herb-Rhubarb network was generated.

2.5. Molecular docking verification

The top three Rhubarb active ingredients in the drug-ingredient-gene network, ranked by node degree, were downloaded from PubChem for their 3D structures. Based on the PPI interactions, the top five core genes with median and degree values above the mean were selected. The 3D structures of corresponding macromolecules were downloaded from the Protein Data Bank (PDB), using X-ray resolution between 1.0 and 2.0 and specifying human species. Macromolecular proteins were deionized and the original ligands were removed using AutoDockTools 1.5.6 software.AutoDock Vina 4.2 was used to evaluate the free binding energy, and PyMOL was employed for visualization of binding sites.

3. Results

3.1. Collection the targets information of AS/AAA and rhubarb

In our study, we analyzed dataset of GSE4329 to identify DEGs in AS between 32 disease samples and 32 normal samples. The gene expression levels of the 64 samples were found to be highly concentrated within the range of [4, 8]. Therefore, we were able to directly process the data without normalization (Fig. 2A). Using a significance threshold of $P < 0.01$, we obtained 5788 DEGs between 32 disease AS samples and 32 normal samples (Supplementary Table S1). Additionally, by utilizing the Disgenet database and considering a SCORE >0.01, we identified 226 potential target genes for AAA (Supplementary Table S2).

A total of 110 candidate disease targets were identified by intersecting the two datasets (Supplementary Table S3). Of these, 38 genes were down-regulated and 72 genes were up-regulated in AS (Fig. 2B and C). The top 5 up-regulated and down-regulated DEGs were visualized using R (Supplementary Table S4).After conducting further observations, statistical significance was subsequently evaluated. (Fig. 2D).

Using the TCMSP database and searching for the keyword "DaHuang", we identified 92 chenmical components of Rhubarb. These components were then screened based on utilizability (OB) $\geq$ 30 % and drug similarity (DL)$\geq$ 0.18, resulting in the identification of 16 effective components (Table 1 and Supplementary Table S5). After removing duplicates and target genes with a probability equal to zero, we obtained 310 target genes(Supplementary Table S6).

By intersecting the 110 disease candidate genes with the target genes of Rhubarb using a Venny diagram (Fig. 2E), we identified 23 intersected targets (Table 2).

The drug-component-intersecting gene network was constructed by Cytoscape 3.9.1 with 12 components, 23 targets, 36 nodes, and 47 edges (Fig. 2F). In the network, the center node is represented in red, representing Rhubarb, while the active components of rhubarb are shown in yellow, and the target genes are displayed in green. The amount of edges attached to each node indicates its interaction complexity. According to the size of the nodes and the ranking of their degrees, the three core ingredients of rhubarb for treating AS/AAA are rhein (rhubarbic acid), aloe-emodin, and physciondiglucoside (rhubarb glucoside) (Supplementary Table S7).

3.2. PPI protein interaction network, core gene screening results

The 23 cross-targets were imported into the STRING database, resulting in a network of 23 nodes and 103 edges (Fig. 3A and B). The results were analyzed using the CytoNCA plugin considering the network's topological properties. Key nodes with median and degree values higher than the average (median of 11 and degree of 18) were filtered to identify the core genes, including TNF, IL-1β, MMP9, TP53, PPARG, and five others (Fig. 3C and Supplementary Table S8).

3.3. GO function enrichment analysis results

The 23 intersecting target genes were involved in a total of 174 biological processes (all $P < 0.1$)(Supplementary Table S9). For the enrichment analysis for MF, BP, and CC, the functional signals with the top 20 P-values were considered (Fig. 4A–C). The top 3 enriched BP terms were Extracellular matrix catabolism, collagenolytic metabolic processes, and positive regulation of gene

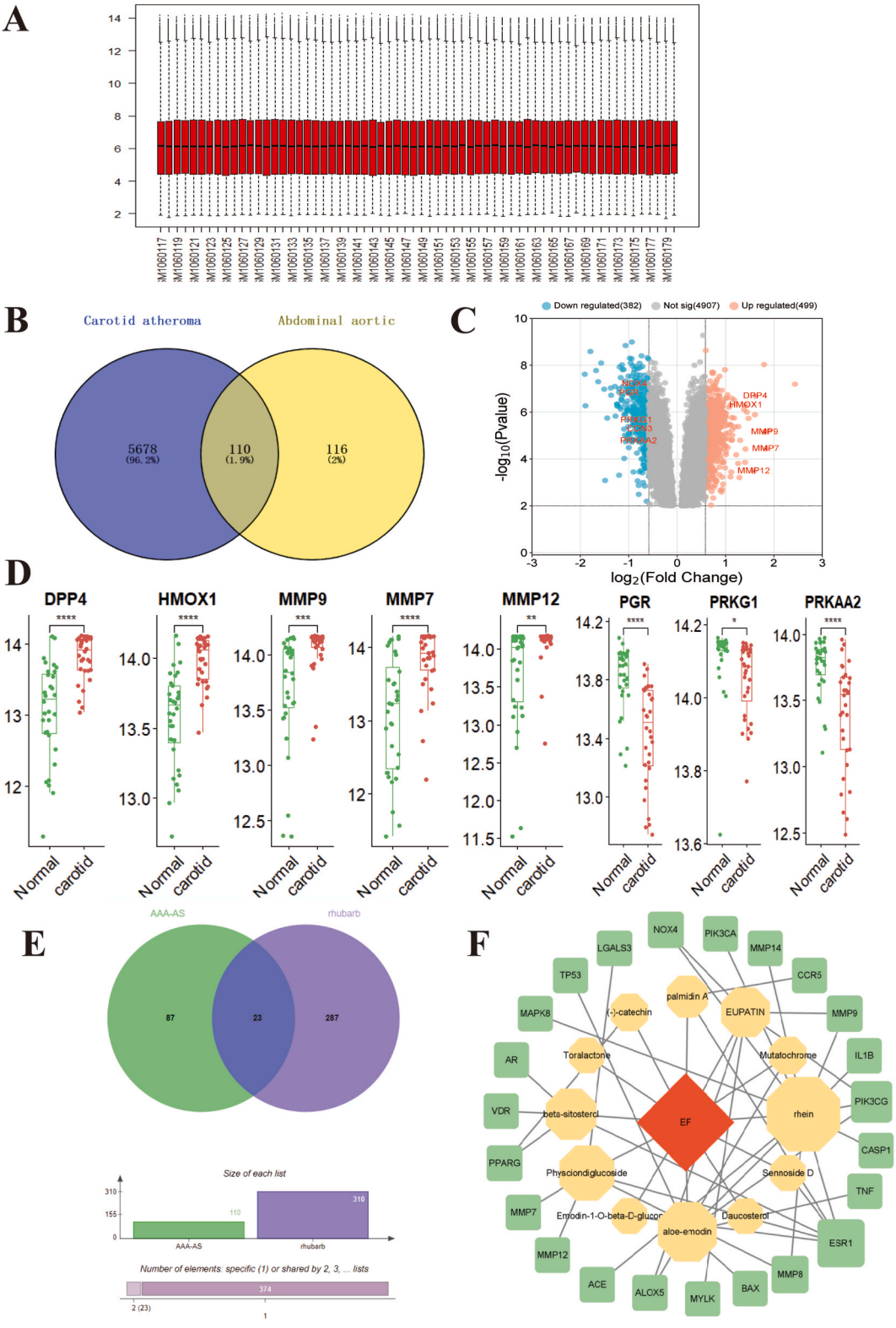

(caption on next page)

Fig. 2. Collection the targets information of AS/AAA and Rhubarb. (A).Boxplot-observation of the expression matrix of genes in the sample. (B). Venn diagram of the 110 common targets between the disease targets of AS and AAA. (C).Differential genes volcano map shows the gene distribution in disease samples. Red and Blue represent up regulated genes and down regulated genes, respectively, whereas grey indicates no significant difference. (D).Gene expression maps to observe the expression of target genes in normal and diseased samples.(E)Venn diagram of the 23 common targets between the active compounds targets of Rhubarb and the disease targets of AS/AAA. (F)Herb–compound–target network.Red for rhubarb, yellow for active ingredient, green for herb genes.The edges represent the interaction between compounds and targets, and the node size is proportional to the degree of interaction.

Table 1
16 effective active components.

Molecular number	Compound name	OB/%	DL
MOL002235	EUPATIN	50.8	0.41
MOL002251	Mutatochrome	48.64	0.61
MOL002259	Physciondiglucoside	41.65	0.63
MOL002260	Procyanidin B-5,3′-O-gallate	31.99	0.32
MOL002268	rhein	47.07	0.28
MOL002276	Sennoside E	50.69	0.61
MOL002280	Torachrysone-8-O-beta-D-(6′-oxayl)-glucoside	43.02	0.74
MOL002281	Toralactone	46.46	0.24
MOL002288	Emodin-1-O-beta-D-glucopyranoside	44.81	0.8
MOL002293	Sennoside D	61.06	0.61
MOL002297	Daucosterol	35.89	0.7
MOL002303	palmidin A	32.45	0.65
MOL000358	beta-sitosterol	36.91	0.75
MOL000471	aloe-emodin	83.38	0.24
MOL000554	gallic acid-3-O-(6′-O-galloyl)-glucoside	30.25	0.67
MOL000096	(−)-catechin	49.68	0.24

Table 2
23 intersected targets.

Number	Gene	Number	Gene	Number	Gene	Number	Gene	Number	Gene
1	NOX4	6	ALOX5	11	LGALS3	16	CCR5	21	BAX
2	PIK3CG	7	MMP7	12	PIK3CA	17	MAPK8	22	TP53
3	MYLK	8	ACE	13	MMP8	18	IL1B	23	ESR1
4	CASP1	9	AR	14	TNF	19	MMP14		
5	MMP9	10	PPARG	15	MMP12	20	VDR		

expression. The highly enriched MF terms were Extracellular milieu, cytoplasm, and cytosol. In addition, the CC terms comprised endopeptidase activity, zinc ion binding, and metalloendopeptidase activity (Fig. 4D).

3.4. KEGG pathway enrichment analysis results

Twenty-three intersecting target genes were involved in 85 pathways ($P < 0.05$)(Supplementary Table S10). Top 20 signaling pathways, determined by P value, were selected for KEGG pathway enrichment analysis on the acquired genes. The major pathways obtained from the screening included Lipids and atherosclerosis (Fig. 5A and B)

The results of KEGG enrichment analysis were used to construct component-target-pathway networks, comprising 57 nodes and 98 edges(Fig. 5C). Additionally, a Sankey diagram (Fig. 5D) was created using a free online platform (http://www.bioinformatics.com.cn) to visualize the connections between target genes and enriched pathways.

KEGG enrichment results suggest that Rhubarb may treat AS/AAA through lipid and atherosclerosis signaling pathways. The "pathview" tool was used to visualize the KEGG pathway (Fig. 5E).

3.5. Results of molecular docking

Table 3 provides information on the binding energies (kcal/mol) of the main targets and active compounds. The free binding energies of the docking results ranged from −4.6 to 2.05 kcal/mol indicating stable binding.Specifically, the free binding energy of IL-1β with rhein was −4.6 kcal/mol. The bound cluster region is the HZ2 residue within the IL-1β LYS103 region (Fig. 6A)

Based on the molecular docking results, rhein exhibits strong binding activity with TP53, while aloe-emodin shows strong binding with IL-1β, PPARG, and TNF (Fig. 6B–E). Therefore, these compounds are considered as potential drug molecules. However, it should be noted that further experimental verification is required for these herbal compounds.

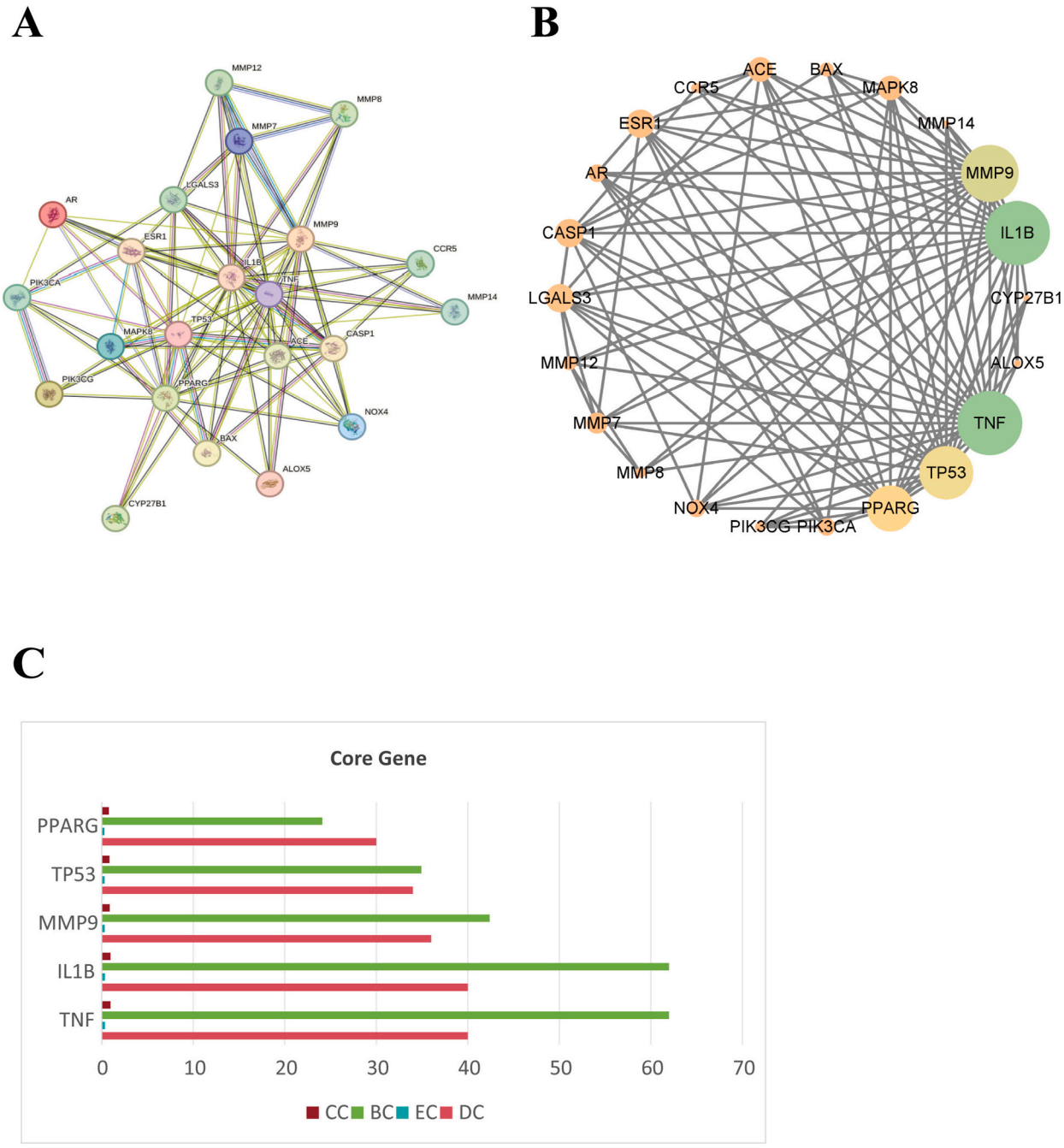

Fig. 3. Identification of candidate targets via protein-protein interaction (PPI) analysis.(A) The process of topological screening for the PPI network. The 23 core targets was obtained by screening 103 edges. (B)The hub genes were selected from the PPI network using the CytoNCA.The node color was from pale orange to green, and the corresponding degree gradually larger. (C)Screening core genes by Degree, Closeness, Betweenness, Eigenvector using CytoNCA plugin, key nodes with median and degree values greater than the mean (median of 11, degree of 18), including TNF, IL-1β, MMP9, TP53, PPARG, 5 core genes.

4. Discussion

AS/AAA is a prevalent cardiovascular disorder resulting from a spectrum of pathological alterations triggered by aortic vascular injury, as documented in numerous studies [22]; [23]. The etiology of AS/AAA is multifaceted, encompassing inflammation, cellular matrix breakdown, oxidative stress, and phenotypic transformations in smooth muscle cells [22]; [23]. These pathological changes collectively contribute to vascular remodeling, culminating in detrimental health outcomes [24]. Amidst this complex pathological

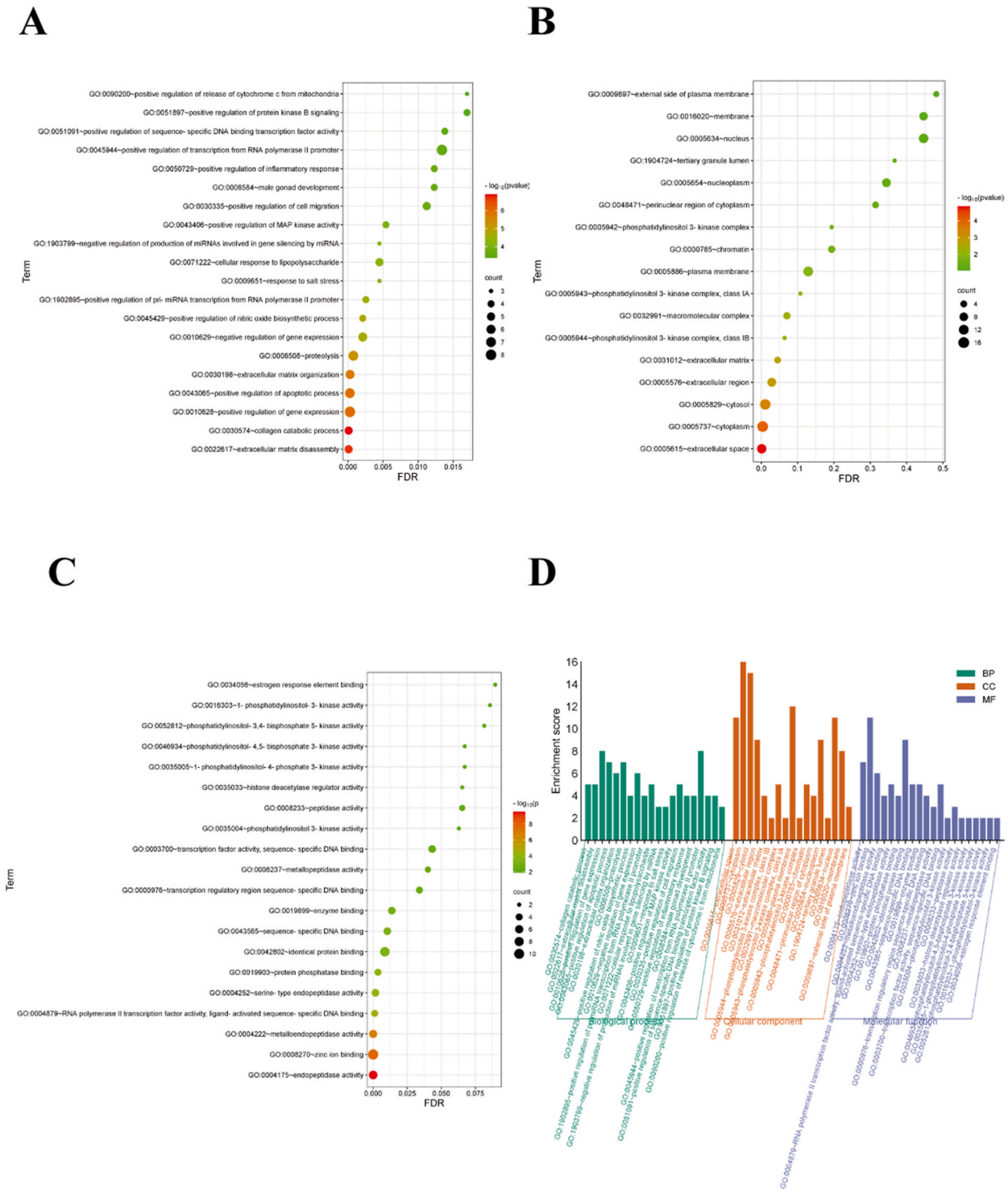

Fig. 4. Results of GO enrichment analysis. (A) Bubble chart of the biological process category terms from GO enrichment analysis. (B) Bubble chart of the cellular component category terms from GO enrichment analysis. (C) Bubble chart of the molecular function category terms from GO enrichment analysis. The X-axis and Y axis show the gene ratios and full names of the processes, respectively, and the color and size of each bubble represent the P value and gene count, respectively; the subsequent bubble charts are presented similarly. (D) Biological process (BP) terms, cellular component (CC) terms, and molecular function (MF) terms of GO enrichment analysis are shown as green, orange, and purple bars, respectively.

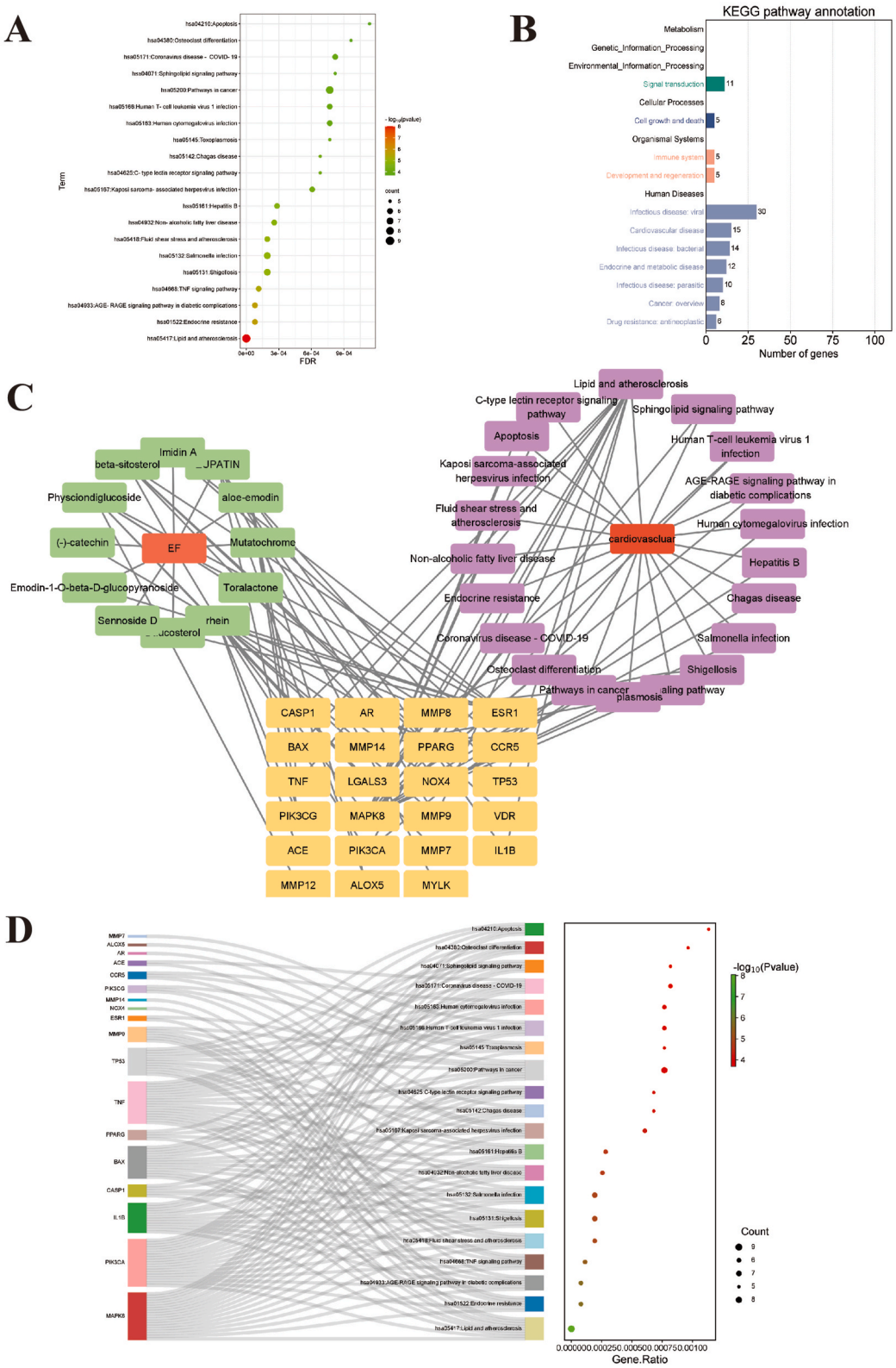

Fig. 5. Results of KEGG enrichment analysis and key pathway network construction. (A) The bubble chart of the top 20 pathways based on KEGG enrichment analysis. (B) The KEGG type of the top 20 pathways based on KEGG enrichment analysis. (C) The compound–target–pathway network implicated in the mechanism of rhubarb in AS/AAA treatment. The yellow nodes represent the targets; the green nodes represent the compounds,

whereas the purple nodes represent the pathways. (D) The sankey diagram of the KEGG pathway analysis. The left rectangle nodes of the sankey diagram represent the therapeutic targets, the right rectangle nodes of the sankey diagram represent the KEGG pathways, and the lines represent the ownership of targets and pathways. (E) Distribution of key targets in the Lipids and atherosclerosis signaling pathways.The putative targets and the genes implicated in the pathway are shown in red.

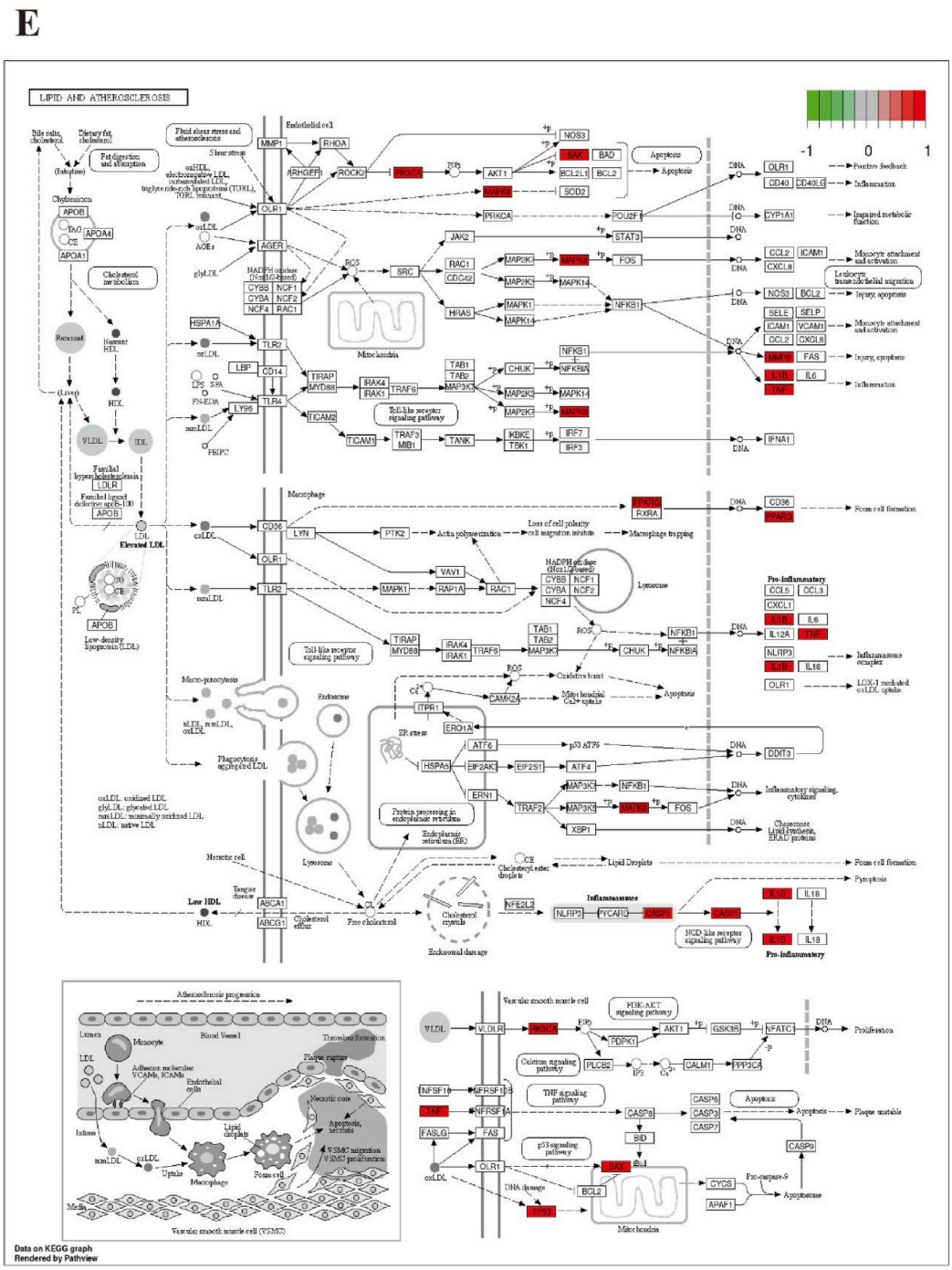

Fig. 5. (*continued*).

landscape, Rhubarb has garnered attention as a promising therapeutic agent for cardiovascular diseases. Nonetheless, the precise active components of Rhubarb and the underlying mechanisms of its anti-inflammatory efficacy remain elusive [25].

To bridge this knowledge gap, we employed a network pharmacology approach to identify potential targets of Rhubarb in treating AS/AAA. This comprehensive methodology integrates systems biology principles with pharmacological data to elucidate complex

Table 3
Binding energies of key targets and active compounds.

Ingredient	Binding energy/(kcal.mol^{-1})				
	MMP9	IL-1β	TNF	TP53	PPARG
Rhein	−3.13	−4.6	−3.48	−4.48	−3.03
Aloe-emodin	−3.11	−4.14	−3.92	−3.42	−4.05
Physciondiglucoside	0.11	−0.07	−0.22	−0.67	2.05

drug-target interactions. Through meticulous validation via molecular docking techniques, we aimed to confirm the predicted interactions and gain deeper insights into the mechanisms of Rhubarb's action. Our findings provide a solid foundation for future research endeavors aimed at harnessing the therapeutic potential of rhubarb in addressing the challenges posed by AS/AAA and related cardiovascular disorders.

Sixteen active compounds of rhubarb were screened from the TCMSP database using ADME principle. Subsequently, 5788 AS disease targets were included from the GEO database and 226 AAA disease targets from the Disgenet database. In total, we identified 110 putative rhubarb-AS/AAA targets. Based on the TCM-ingredient-target network, the top three active ingredients were screened according to the rank of degree value are rhein, aloe-emodin, and physciondiglucoside. Previous research supports the efficacy of these compounds in the treatment of cardiovascular diseases. Rhein has been found to improve high-fat-induced endothelium-dependent diastolic dysfunction in the aorta, reduce vascular stiffness, improves vascular elasticity, and lower inflammation levels in the aorta ([26]; [27]; [28]; [29]). Aloe-emodin can ameliorate Ang II-induced hypertension and damage to vascular endothelial junction proteins. The mechanism is closely linked to the promotion of NLRP 3 ubiquitination-mediated activation of NLRP 3 inflammatory bodies ([30–33]). The rhodopsin derivative physciondiglucoside attenuates high glucose-induced vascular inflammatory responses by inhibiting NF-κB activation, leukocyte adhesion, and hyperosmolarity ([34–36]). The therapeutic effects of the active compounds in rhubarb on cardiovascular disease have been well-establishe.

This study utilized bioinformatics approaches to comprehensively explore the involvement of five key targets: TNF, IL-1β, MMP9, TP53, and PPARG. Specifically, TNF, IL-1β, and MMP9 emerged as significant players in the development of AS/AAA, demonstrating strong interconnectedness within the clustering network. Through GO and KEGG enrichment analyses, it was revealed that Rhubarb may exert its anti-AS and anti-AAA effects by modulating diverse biological processes. These terms include extracellular matrix catabolism, extracellular environment regulation, endopeptidase activity, lipid metabolism, as well as atherosclerosis-related mechanisms. Furthermore, Rhubarb demonstrates antiviral, anti-inflammatory, and immunomodulatory properties, along with its influence on pertinent signaling pathways. These findings provide valuable insights into the multifaceted therapeutic potential of Rhubarb in addressing AS/AAA and related disorders.

Molecular docking was employed to assess the docking ability of five key target proteins (TNF, IL-1β, MMP9, TP53 and PPARG) with active compounds obtained from TCMSP, namely rhein, aloe-emodin, and physciondiglucoside. The docking results revealed binding affinities ranging from −4.6 to 2.05 kcal/mol, indicating high docking capacities of all targets with the active compounds. Among the five target proteins, IL-1β and TP53 exhibited the lowest binding affinities.

As a result, the full functionality of Rhubarb remains somewhat elusive and cannot be precisely predicted solely based on the current findings. Therefore, further experimental and clinical validation is warranted to definitively ascertain the effects of Rhubarb and ensure its safe and effective use.

5. Conclusion

In summary, this study systematically examined the pharmacological and molecular mechanisms of Rhubarb in treating AS/AAA using bioinformatics, network pharmacology, and molecular docking. The key findings indicate that rhubarbic acid, aloe barbadensis, and rhubarb glucoside are its primary active compounds, reducing vascular damage, oxidative stress, and inflammation through multiple targets, offering novel insights for exploring Chinese medicine pharmacology.

CRediT authorship contribution statement

Huilin Xu: Writing – original draft, Data curation, Conceptualization. **Jun Huang:** Funding acquisition, Formal analysis. **Youjie Zeng:** Software, Resources, Methodology. **Xia Wang:** Resources. **Huilin Lian:** Resources. **Siyi Zhang:** Formal analysis. **Ren Guo:** Visualization, Supervision, Investigation.

Data availability statement

The raw data for this article are included in the article or supplementary material; for further inquiries, please contact the corresponding author.

Funding

This project was financially supported by the Natural Science Foundation of Hunan Province (Grant No. 2021JJ31004).

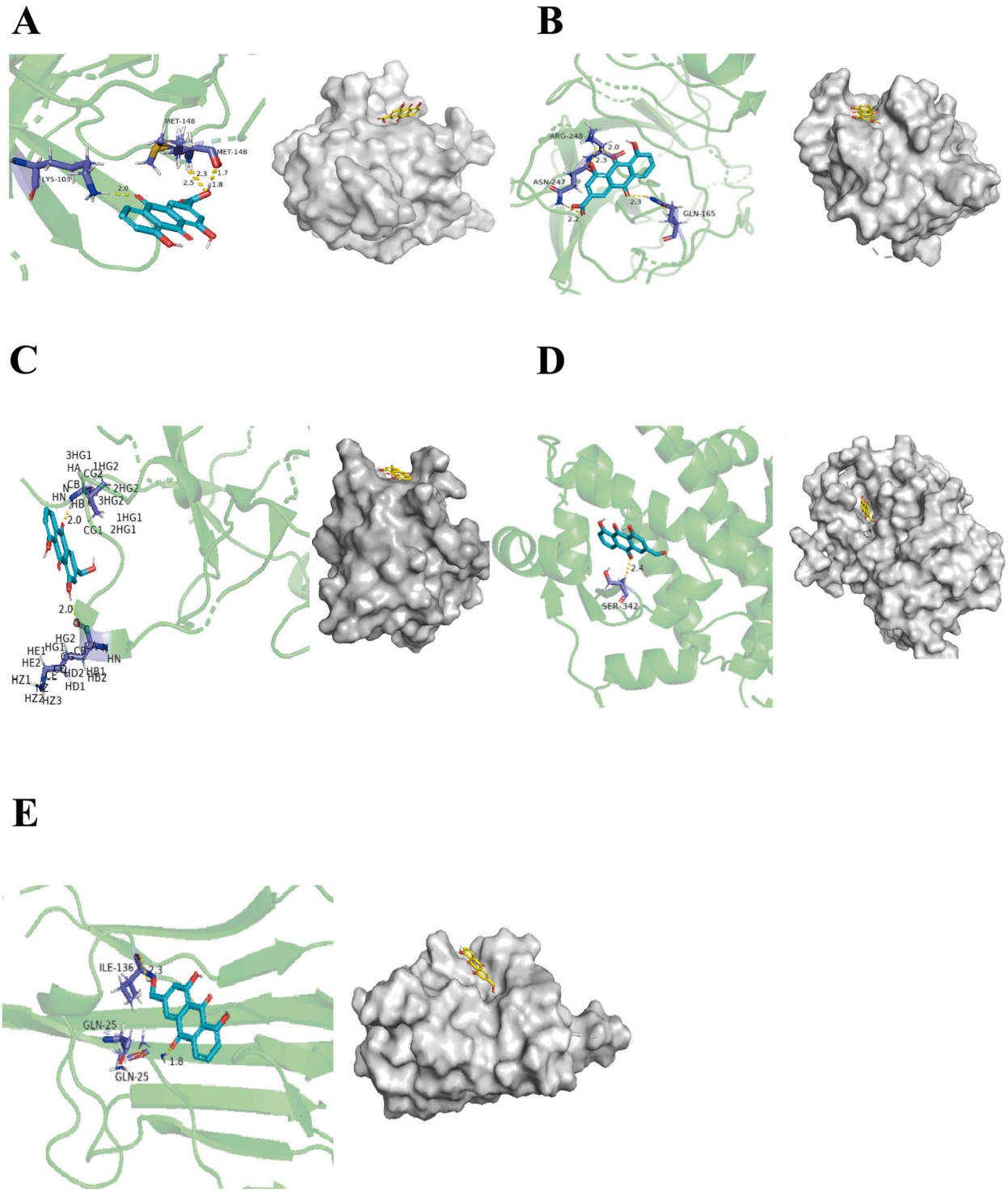

Fig. 6. Docking patterns of key targets and specific active compounds.(A) rhein with IL-1β.(B) rhein with TP53.(C) aloe-emodin with IL-1β,(D)aloe-emodin PPARG (E)aloe-emodin with TNF.

Declaration of competing interest

The authors have declared that no conflict interest exists.

The authors declare that they have no known competing financial interests or personal relationships that could have appeared to influence the work reported in this paper.

Acknowledgments

We would like to thank all the members for their efforts, the mentors for their careful guidance and the platform provided by the Third Xiangya Hospital of Central South University.

Appendix A. Supplementary data

Supplementary data to this article can be found online at https://doi.org/10.1016/j.heliyon.2025.e41906.

References

[1] P. Chatterjee, K.A. Martin, A concept of "Athero-Oncology": tumor-like smooth muscle cells drive atherosclerosis, Circulation 149 (24) (2024) 1899–1902, https://doi.org/10.1161/circulationaha.124.069446.
[2] G. Zhu, L. Cao, J. Wu, M. Xu, Y. Zhang, M. Wu, J. Li, Co-morbid intersections of cancer and cardiovascular disease and targets for natural drug action: reprogramming of lipid metabolism, Biomed. Pharmacother. 176 (2024) 116875, https://doi.org/10.1016/j.biopha.2024.116875.
[3] M. Carlstrom, E. Weitzberg, J.O. Lundberg, Nitric oxide signaling and regulation in the cardiovascular system: recent advances, Pharmacol. Rev. (2024), https://doi.org/10.1124/pharmrev.124.001060.
[4] M. Mori, A. Sakamoto, R. Kawakami, L. Guo, L. Slenders, J.V. Mosquera, A.V. Finn, CD163(+) macrophages induce endothelial-to-mesenchymal transition in atheroma, Circ. Res. (2024), https://doi.org/10.1161/circresaha.123.324082.
[5] Q. Zhu, P.E. Scherer, Ceramides and atherosclerotic cardiovascular disease: a current perspective, Circulation 149 (21) (2024) 1624–1626, https://doi.org/10.1161/circulationaha.123.065409.
[6] M.J. Cho, M.R. Lee, J.G. Park, Aortic aneurysms: current pathogenesis and therapeutic targets, Exp. Mol. Med. 55 (12) (2023) 2519–2530, https://doi.org/10.1038/s12276-023-01130-w.
[7] H.S. Lu, R.E. Temel, M.G. Levin, S.M. Damrauer, A. Daugherty, Research advances in abdominal aortic aneurysms: triglyceride-rich lipoproteins as a therapeutic target, Arterioscler. Thromb. Vasc. Biol. 44 (6) (2024) 1171–1174, https://doi.org/10.1161/atvbaha.124.320146.
[8] D. Domagała, K. Data, H. Szyller, M. Farzaneh, P. Mozdziak, S. Woźniak, B. Kempisty, Cellular, molecular and clinical aspects of aortic aneurysm-vascular physiology and pathophysiology, Cells 13 (3) (2024), https://doi.org/10.3390/cells13030274.
[9] T. Troëng, F. Lundgren, VASCUNET and abdominal aortic aneurysm: what's next? Eur. J. Vasc. Endovasc. Surg. (2024) https://doi.org/10.1016/j.ejvs.2024.05.007.
[10] Y. Lei, X. Fu, M. Chen, Y. Yi, P. Mao, L. Peng, Z. Qu, Dahuang-Taoren, a botanical drug combination, ameliorates adenomyosis via inhibiting Rho GTPases, Front. Pharmacol. 14 (2023) 1089004, https://doi.org/10.3389/fphar.2023.1089004.
[11] Q. Zhang, J. Liu, R. Li, R. Zhao, M. Zhang, S. Wei, C. Wu, A network pharmacology approach to investigate the anticancer mechanism and potential active ingredients of Rheum palmatum L. Against lung cancer via induction of apoptosis, Front. Pharmacol. 11 (2020) 528308, https://doi.org/10.3389/fphar.2020.528308.
[12] X. He, J. Liang, X. Li, Y. Wang, X. Zhang, D. Chen, S. Wang, Dahuang zhechong pill ameliorates hepatic fibrosis by regulating gut microbiota and metabolites, J. Ethnopharmacol. 321 (2024) 117402, https://doi.org/10.1016/j.jep.2023.117402.
[13] S. Huang, X. Wang, X. Xie, Y. Su, Z. Pan, Y. Li, L. Zhou, Dahuang Mudan decoction repairs intestinal barrier in chronic colitic mice by regulating the function of ILC3, J. Ethnopharmacol. 299 (2022) 115652, https://doi.org/10.1016/j.jep.2022.115652.
[14] M.Y. Qin, S.Q. Huang, X.Q. Zou, X.B. Zhong, Y.F. Yang, Y.T. Zhang, Z.G. Huang, Drug-containing serum of rhubarb-astragalus capsule inhibits the epithelial-mesenchymal transformation of HK-2 by downregulating TGF-β1/p38MAPK/Smad2/3 pathway, J. Ethnopharmacol. 280 (2021) 114414, https://doi.org/10.1016/j.jep.2021.114414.
[15] S. Xiao, Z. Zhang, M. Chen, J. Zou, S. Jiang, D. Qian, J. Duan, Xiexin Tang ameliorates dyslipidemia in high-fat diet-induced obese rats via elevating gut microbiota-derived short chain fatty acids production and adjusting energy metabolism, J. Ethnopharmacol. 241 (2019) 112032, https://doi.org/10.1016/j.jep.2019.112032.
[16] J. Cai, Y. Zhan, K. Huang, S. Han, Z. Lin, R. Chen, S. Li, Integration of network pharmacology and proteomics analysis to identify key target pathways of Ginsenoside Re for myocardial ischemia, Phytomedicine (2024) 155728, https://doi.org/10.1016/j.phymed.2024.155728.
[17] B. Li, J. Bao, Y. Huang, J. Liu, X. Yan, Q. Zou, Dual-integrin-targeted supramolecular peptide nanoarchitectonics for enhanced hepatic delivery and antifibrotic therapy, Small (2024) e2409038, https://doi.org/10.1002/smll.202409038.
[18] G. Pacheco, A.L.F. Lopes, A.P. Oliveira, W.R.M. Corrêa, L.D.B. Lima, M. Souza, J.V.R. Medeiros, Comprehensive analysis of gastrointestinal side effects in COVID-19 patients undergoing combined pharmacological treatment with azithromycin and hydroxychloroquine: a systematic review and network meta-analysis, Crit. Rev. Toxicol. (2024) 1–14, https://doi.org/10.1080/10408444.2024.2348169.
[19] G. Luo, T. Ming, L. Yang, L. He, T. Tao, Y. Wang, Modulators targeting protein-protein interactions in Mycobacterium tuberculosis, Microbiol. Res. 284 (2024) 127675, https://doi.org/10.1016/j.micres.2024.127675.
[20] J.M. Paggi, A. Pandit, R.O. Dror, The art and science of molecular docking, Annu. Rev. Biochem. (2024), https://doi.org/10.1146/annurev-biochem-030222-120000.
[21] Z. Jin, Z. Wei, Molecular simulation for food protein-ligand interactions: a comprehensive review on principles, current applications, and emerging trends, Compr. Rev. Food Sci. Food Saf. 23 (1) (2024) e13280, https://doi.org/10.1111/1541-4337.13280.
[22] F. Crea, Focus on translational vascular biology: new therapeutic targets in hypertension, aortic aneurysm, and atherosclerosis, Eur. Heart J. 44 (29) (2023) 2645–2649, https://doi.org/10.1093/eurheartj/ehad481.
[23] F. Crea, Focus issue on vascular biology and medicine spanning from management of stroke to new therapeutic targets in aortic dissection and pulmonary hypertension, Eur. Heart J. 44 (14) (2023) 1193–1196, https://doi.org/10.1093/eurheartj/ehad198.
[24] Q. Yang, F. Saaoud, Y. Lu, Y. Pu, K. Xu, Y. Shao, X. Yang, Innate immunity of vascular smooth muscle cells contributes to two-wave inflammation in atherosclerosis, twin-peak inflammation in aortic aneurysms and trans-differentiation potential into 25 cell types, Front. Immunol. 14 (2023) 1348238, https://doi.org/10.3389/fimmu.2023.1348238.

[25] Q. Liu, X. Ba, L. Han, J. Yan, Z. Chen, K. Qin, P. Shen, Dahuang-Wumei decoction protects against hepatic encephalopathy in mice: behavioural, biochemical, and molecular evidence, Phytomedicine 128 (2024) 155419, https://doi.org/10.1016/j.phymed.2024.155419.
[26] H.R.P. Carmo, A.R. Castillo, I. Bonilha, E.I.L. Gomes, J. Barreto, F.A. Moura, A.C. Sposito, Diacerein reduces inflammasome activation and SARS-CoV-2 virus replication: a proof-of-concept translational study, Front. Pharmacol. 15 (2024) 1402032, https://doi.org/10.3389/fphar.2024.1402032.
[27] Y. Chen, Y. Tu, J. Cao, Y. Wang, Y. Ren, Rhein alleviates doxorubicin-induced myocardial injury by inhibiting the p38 MAPK/HSP90/c-Jun/c-Fos pathway-mediated apoptosis, Cardiovasc. Toxicol. 24 (11) (2024) 1139–1150, https://doi.org/10.1007/s12012-024-09917-7.
[28] W. Zhao, B. Li, J. Hao, R. Sun, P. He, H. Lv, Y. Han, Therapeutic potential of natural products and underlying targets for the treatment of aortic aneurysm, Pharmacol. Ther. 259 (2024) 108652, https://doi.org/10.1016/j.pharmthera.2024.108652.
[29] A. Zhao, X. Liu, X. Chen, S. Na, H. Wang, X. Peng, L. Li, Aqueous extract of rhubarb promotes hepatotoxicity via facilitating PKM2-mediated aerobic glycolysis in a rat model of diethylnitrosamine-induced liver cancer, Drug Des Devel Ther 18 (2024) 4497–4510, https://doi.org/10.2147/dddt.S476273.
[30] Q. Chen, K.T. Li, S. Tian, T.H. Yu, L.H. Yu, H.D. Lin, D.Q. Bai, Photodynamic therapy mediated by aloe-emodin inhibited angiogenesis and cell metastasis through activating MAPK signaling pathway on HUVECs, Technol. Cancer Res. Treat. 17 (2018) 1533033818785512, https://doi.org/10.1177/1533033818785512.
[31] M. Sapkota, S.K. Shrestha, M. Yang, Y.R. Park, Y. Soh, Aloe-emodin inhibits osteogenic differentiation and calcification of mouse vascular smooth muscle cells, Eur. J. Pharmacol. 865 (2019) 172772, https://doi.org/10.1016/j.ejphar.2019.172772.
[32] J. Wu, X. Ke, W. Wang, H. Zhang, N. Ma, W. Fu, Z. Zhang, Aloe-emodin suppresses hypoxia-induced retinal angiogenesis via inhibition of HIF-1α/VEGF pathway, Int. J. Biol. Sci. 12 (11) (2016) 1363–1371, https://doi.org/10.7150/ijbs.16334.
[33] C. Xu, C. Yin, S. Wang, Effect of aloe-emodin on expression of proliferating cell nuclear antigen of vascular smooth muscle cells in culture after arterial injury, Chin Med J (Engl) 114 (6) (2001) 571–576.
[34] C. Chen, J. Gu, J. Wang, Y. Wu, A. Yang, T. Chen, Z. Liu, Physcion 8-O-β-glucopyranoside ameliorates liver fibrosis through inflammation inhibition by regulating SIRT3-mediated NF-κB P65 nuclear expression, Int Immunopharmacol 90 (2021) 107206, https://doi.org/10.1016/j.intimp.2020.107206.
[35] J. Geng, G. Zhou, S. Guo, C. Ma, J. Ma, Underlying mechanism of traditional herbal formula chuang-ling-ye in the treatment of diabetic foot ulcer through network pharmacology and molecular docking, Curr Pharm Des 30 (6) (2024) 448–467, https://doi.org/10.2174/0113816128287155240122121553.
[36] M. Wang, J. Xu, Y. Zhang, N. Yang, W. Ge, R. Song, Integrated multiplatform-based metabonomics and network analysis to explore the mechanism of Polygonum cuspidatum on hyperlipidemia, J Chromatogr B Analyt Technol Biomed Life Sci 1176 (2021) 122769, https://doi.org/10.1016/j.jchromb.2021.122769.